FULL PAPER

Dalton
www.rsc.org/dalton

Macrocyclic ligand design. Structure–function relationships involving the interaction of pyridinyl-containing, oxygen–nitrogen donor macrocycles with selected transition and post transition metal ions on progressive *N*-benzylation of their secondary amines†

Jason R. Price,[a] Marina Fainerman-Melnikova,[a] Ronald R. Fenton,[a] Karsten Gloe,[b] Leonard F. Lindoy,*[a] Torsten Rambusch,[a,b] Brian W. Skelton,[c] Peter Turner,[a] Allan H. White[c] and Kathrin Wichmann[a,b]

[a] *Centre for Heavy Metals Research, School of Chemistry, the University of Sydney, NSW 2006, Australia*

[b] *Institut für Anorganische Chemie, TU Dresden, 01062 Dresden, Germany*

[c] *Chemistry M313, The University of Western Australia, Crawley, WA 6009, Australia*

Received 12th August 2004, Accepted 14th September 2004
First published as an Advance Article on the web 8th October 2004

Structure–function relationships underlying the interaction of progressively *N*-benzylated N_4O_2-donor macrocycles with cobalt(II), nickel(II), copper(II), zinc(II), cadmium(II), silver(I) and lead(II) have been probed using a range of techniques that include X-ray diffraction, DFT computations, solvent extraction, potentiometric stability constant determinations and competitive membrane transport experiments. Collectively, the results indicate that *N*-benzylation of the secondary amine donor groups of the parent macrocyclic ring results in an enhanced tendency towards selectivity for silver(I) relative to the other six metals investigated. The observed behaviour serves as additional exemplification of the previously proposed concept of selective 'detuning' as a mechanism for metal ion discrimination.

Introduction

Metal-ion recognition by organic substrates is an area of fundamental importance to numerous aspects of both chemistry and biochemistry. In previous studies our group has investigated the effect on *N*-alkylation of secondary nitrogen atoms in both mixed-donor[1–3] and N_4-donor[4] macrocyclic ligands on their metal-ion recognition properties towards the following transition and post-transition metal ions: cobalt(II), nickel(II), copper(II), zinc(II), cadmium(II), lead(II) and silver(I). The aim of these studies has been to probe structure/function effects in terms of metal-ion discrimination behaviour. Over several such ligand systems it has been documented that there is a tendency for *N*-benzylation to reduce the affinity (often very significantly) of such ligand systems for the first six of the above metal ions while the affinity for silver(I) remains much less affected. We have termed behaviour of this type 'selective detuning'.[5] The latter represents a potential metal ion discrimination mechanism that has received little attention by others. Nevertheless, in this context it needs to be noted that a limited number of examples of *N*-alkylation leading to enhanced metal ion selectivity and related behaviour have been reported previously.[6,7] For example, while alkylation of a secondary amine generally results in a reduction of its metal ion affinity due to steric factors, it has been documented that tertiary amines sometimes bind more strongly to silver(I) compared with secondary amines and that the relative affinities can be solvent dependant.[6] Similarly, the *N*-methylation of secondary amines has been shown by Meyerstein *et al.*[8] to favour stabilisation of the monovalent state of copper relative to its divalent state as exemplified by the electrochemical behaviour of copper(I) and copper(II) in the presence of the tetra-*N*-methylated cyclam derivative *versus* parent cyclam. A variety of influences have been proposed to account for such behaviour, with solvation effects predicted to be dominant, lower oxidation states are expected to be stabilised on *N*-alkylation.

We now report an extension of our prior studies involving the interaction of the seven metal-ion series mentioned above with the progressively *N*-benzylated, O_2N_4-donor macrocycles **1**–**6**, each incorporating a 20-membered macrocyclic ring. The related 17-membered ring species of type **7** have been the focus of a prior study by us.[2] It was of particular interest in the present investigation to probe the effect of the larger ring and the presence of a pyridyl nitrogen donor in each of **1**–**6** on the relative 'detuning' behaviour towards the metal-ion series mentioned above.

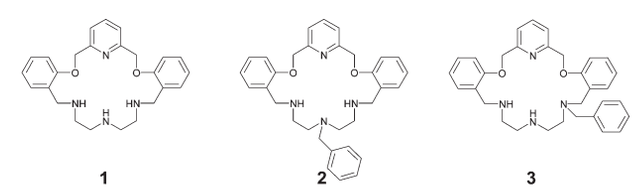

1 **2** **3**

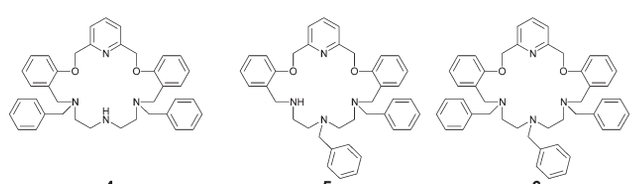

4 **5** **6**

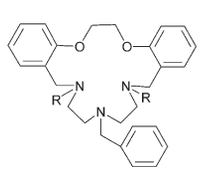

7 (R = H or Benzyl)

† Electronic supplementary information (ESI) available: Table S1 (coordinated anion and other geometries $[M(\mathbf{2})(NO_3)_2]$ (M = Co, Zn, Cd, Ni)) and Table S2 (ligand conformational descriptors); Fig. S1 (calculated geometry of the lowest found minimum structure of $[Ag(\mathbf{4})]^+$) and Fig. S2 (calculated geometry of the minor disordered component of $[Ag(\mathbf{4})]^+$. See http://www.rsc.org/suppdata/dt/b4/b412437e/

DOI: 10.1039/b412437e

Experimental

All commercial reagents and solvents were of analytical (or HPLC) grade where available. Tetrakis(acetonitrile)copper(I) hexafluorophosphate was synthesized by the literature procedure.[9] The preparation of **1**–**6** has been reported previously.[10]

Physical measurements

UV-VIS spectra were obtained in methanol on a Cary 5E spectrophotomer. A Finnigan LCQ-8 spectrometer was employed for low resolution, positive ion ESMS. X-Band EPR spectra were obtained as the first derivatives from frozen DMF solution at liquid N_2 temperature. A Bruker EMX EPR spectrometer (operating microwave frequency ≈9.3 GHz) equipped with a Bruker EMX 035M NMR gaussmeter coupled with EMX 048T microwave bridge controller and EMX032T field controller for calibration, a Bruker EMX 081 magnet and an ERO 41XG microwave bridge were used. Spectral manipulations and calculations were performed using the WINEPR software package.[11] Magnetic susceptibilities were measured on a Sherwood Scientific magnetic susceptibility balance (Cambridge Research Laboratories).

Potentiometric titrations

The stability constants were determined by potentiometric titration. All reagents were analytical grade, with analytical grade methanol being fractionated and distilled from magnesium/iodine before use. The apparatus consisted of a water-jacketed measuring cell containing a Philips glass electrode (GA-110) and a water-jacketed calomel reference electrode connected by a salt bridge. A solution of base (tetraethylammonium hydroxide) was introduced into the measuring cell by means of a Metrohm dosimat 665 automatic titrator under personal computer control.

The protonation constants for the respective ligands and the corresponding metal stability constants were obtained in 95% methanol (I = 0.1 M, Et_4NClO_4), with the data processed using a local version of MINIQUAD.[12] The titration data for the metal complexation were successfully refined assuming the presence of only 1 : 1 metal–ligand species in solution; in virtually all cases only data corresponding to the lower portions of the titration curves were employed for the calculations in order to avoid complications arising from competing hydrolysis/precipitation at higher pH values. Quoted log K values (see Table 2) are the mean of two or three separate determinations obtained at different metal to ligand ratios (in each case measured on duplicate sets of potentiometric titration apparatus). Unless otherwise specified, all log K values obtained in separate titrations fell within ±0.1 units (and usually within ±0.05 units) of the mean value for a given metal/ligand system.

Liquid–liquid extraction experiments

The solvent extraction experiments were carried out at 26 ± 2 °C in polypropylene micro-centrifuge tubes (2 mL) with a phase ratio $V_{(aq)} : V_{(org)}$ of 1 : 1 (each phase 0.5 mL). The aqueous phase contained the metal ion (at 1.0×10^{-4} M), a supporting anion, picric acid (5.0×10^{-3} M) or sodium nitrate (5.0×10^{-3} M), and a selected buffer (used to maintain the chosen pH). The pH of the aqueous phase was checked before and after each experiment. The organic phase contained a known concentration of ligand in chloroform (normally 1.0×10^{-3} M except where variable concentration experiments were employed). All experiments involved mechanical shaking of the vials for 30 min, except for extractions involving cobalt(II) where they were shaken for 3 h. At the end of these periods, the phases were separated, centrifuged (to ensure full phase separation) and then duplicate 100 μL samples of the aqueous and organic phases were removed for analysis. Trial experiments were undertaken in each case to confirm that equilibrium is attained within the respective above time periods.

The metal concentration in both phases was determined radiometrically by means of γ-counting using a NaI(Tl) Scintillation Counter (Cobra II, Canberra-Packard). The following metal isotopes were employed: ^{110m}Ag, ^{65}Zn, ^{60}Co and ^{64}Cu. The values from the duplicate analyses were averaged, then taken as the 'working' concentration in each case.

Membrane transport

The transport experiments employed a 'concentric cell' in which the aqueous source phase (10 mL) and receiving phase (30 mL) were separated by a chloroform phase (50 mL). Details of the cell design have been reported elsewhere.[13] For each experiment both the aqueous phases and the organic phase were stirred separately at 10 rpm; the cell was enclosed by a water jacket and thermostatted at 25 °C. The aqueous source phase was buffered (CH_3CO_2H–CH_3CO_2Na) at pH 4.9 (±0.1) (6.95 mL of 2 M sodium acetate solution and 3.05 mL of 2 M acetic acid made up to 100 mL)[14] and contained an equimolar solution of the nitrate salts of cobalt(II), nickel(II), zinc(II), copper(II), cadmium(II), lead(II) and silver(I), each at a concentration of 1×10^{-2} M. The chloroform phase contained the ligand (1×10^{-3} M), as well as palmitic acid at 4×10^{-3} M. The aqueous receiving phase was buffered (HCO_2H–HCO_2Na) at pH 3.0 ± 0.1 (56.6 mL of 1 M formic acid and 10.0 mL of 1 M sodium hydroxide made up to 100 mL).[14] All transport runs were terminated after 24 hours and atomic absorption spectroscopy was used to determine the amount of metal ion transported over this period. Transport rates (J values) are in mol $(24\ h)^{-1}$. The transport results are quoted as the average values obtained from duplicate runs (maximum error *ca.* ±10% of reported value).

Crystal structure determinations

Full spheres of CCD area-detector diffractometer data were measured (Bruker AXS instrument, ω-scans; monochromatic Mo-Kα radiation, λ = 0.71073 Å; T *ca.* 150 K) yielding $N_{t(total)}$ reflections, merging to N unique (R_{int} cited) after 'empirical'/multiscan absorption correction (proprietary software), N_o with $F > 4\sigma(F)$ being considered 'observed' and used in the full matrix least squares refinement, refining anisotropic thermal parameter forms for the non-hydrogen atoms, $(x, y, z, U_{iso})_H$ being constrained at estimates, unless otherwise stated. Conventional residuals R, R_w on $|F|$ are cited at convergence (weights: $(\sigma^2(F) + 0.0004F^2)^{-1}$). Neutral atom complex scattering factors were used within the Xtal 3.7 program system.[15] Pertinent results are given below and in Tables 3–5 and in Electronic Supplementary Information† Table S1 (Coordinated anion and other geometries [M(**2**)$(NO_3)_2$] (M = Co, Zn, Cd, Ni)) and Table S2 (Ligand conformational descriptors) as well as in Figs. 6–13 (these showing 50% displacement amplitude ellipsoids for the non-hydrogen atoms, hydrogen atoms having arbitrary radii of 0.1 Å).

CCDC reference numbers 247455–247466.

See http://www.rsc.org/suppdata/dt/b4/b412437e/ for crystallographic data in CIF or other electronic format.

Crystal/refinement data. [(**2**)H_2]$(PF_6)(PF_2O_2)\cdot H_2O\cdot CH_3CN \equiv C_{34}H_{43}F_8N_5O_5P_2$, M = 815.7. Monoclinic, space group $P2_1/c$ (C_{2h}^5, No.14), a = 12.0235(6), b = 18.5839(9), c = 17.1673(9) Å, β = 96.688(1)°, V = 3810 Å^3. D_c (Z = 4) = 1.422 g cm^{-3}. μ_{Mo} = 2.0 cm^{-1}; specimen: 0.15 × 0.15 × 0.12 mm; 'T'$_{min/max}$ = 0.87. $2\theta_{max}$ = 75°; N_t = 78600, N = 20042 (R_{int} = 0.028), N_o = 13867; R = 0.055, R_w = 0.065.

Variata. Refinement of $(x,y,z,U_{iso})_H$ throughout establishes the credibility of the solvent complement. The anion assignment is based on refinement and geometrical considerations; the PF_6 anion is modelled with the fluorine atoms disordered over two sets of sites, occupancies 0.875(2) and complement, isotropic displacement parameter forms refined for the minor component.

$[M(\mathbf{2})(NO_3)_2]\cdot 2CH_3OH \equiv C_{34}H_{44}N_6O_{10}M$ (M = Co, Zn, Cd). Monoclinic, space group $P2_1/n$ (C_{2h}^5, No.14 (variant)), $Z = 4$ $(x,y,z,U_{iso})_H$ refined for the Co, Cd adducts.

(*i*) $[Co(\mathbf{2})(NO_3)_2]\cdot 2CH_3OH$. $M = 755.7$. $a = 17.586(2)$, $b = 9.1457(8)$, $c = 23.063(2)$ Å, $\beta = 100.249(2)°$, $V = 3480$ Å^3. $D_c = 1.442$ g cm^{-3}. $\mu_{Mo} = 5.6$ cm^{-1}; specimen: $0.30 \times 0.14 \times 0.11$ mm; 'T'$_{min/max} = 0.95$. $2\theta_{max} = 58°$; $N_t = 64342$, $N = 9231$ ($R_{int} = 0.043$), $N_o = 7094$; $R = 0.042$, $R_w = 0.048$.

(*ii*) $[Zn(\mathbf{2})(NO_3)_2]\cdot 2CH_3OH$. $M = 762.2$. $a = 17.637(4)$, $b = 9.133(2)$, $c = 23.161(4)$ Å, $\beta = 110.049(6)°$, $V = 3505$ Å^3. $D_c = 1.444$ g cm^{-3}. $\mu_{Mo} = 7.7$ cm^{-1}; specimen: $0.14 \times 0.10 \times 0.09$ mm; 'T'$_{min/max} = 0.85$. $2\theta_{max} = 55°$; $N_t = 12819$ (hemisphere), $N = 8070$ ($R_{int} = 0.067$), $N_o = 5492$; $R = 0.055$, $R_w = 0.070$.

(*iii*) $[Cd(\mathbf{2})(NO_3)_2]\cdot 2CH_3OH$. $M = 809.2$. $a = 17.693(2)$, $b = 9.338(1)$, $c = 22.992(3)$ Å, $\beta = 109.128(3)°$, $V = 3589$ Å^3. $D_c = 1.497$ g cm^{-3}. $\mu_{Mo} = 6.7$ cm^{-1}; specimen: $0.28 \times 0.18 \times 0.12$ mm; 'T'$_{min/max} = 0.87$. $2\theta_{max} = 75°$; $N_t = 46795$, $N = 17963$ ($R_{int} = 0.033$), $N_o = 13449$; $R = 0.038$, $R_w = 0.047$.

$[Ag(\mathbf{2})]BF_4 \equiv C_{32}H_{36}AgBF_4N_4O_2$, $M = 703.3$. Monoclinic, space group $P2_1/c$ (C_{2h}^5, No.14), $a = 9.427(1)$, $b = 16.268(2)$, $c = 20.346(3)$ Å, $\beta = 101.348(5)°$, $V = 3059$ Å^3. D_c ($Z = 4$) = 1.527 g cm^{-3}. $\mu_{Mo} = 7.2$ cm^{-1}; specimen: $0.35 \times 0.18 \times 0.11$ mm; 'T'$_{min/max} = 0.87$. $2\theta_{max} = 60°$; $N_t = 38639$, $N = 8774$ ($R_{int} = 0.048$), $N_o = 6659$; $R = 0.049$, $R_w = 0.061$.

$[Ag(\mathbf{4})]PF_6 \equiv C_{39}H_{42}AgF_6N_4O_2P$, $M = 851.6$. Monoclinic, space group $P2_1/c$, $a = 10.362(1)$, $b = 17.501(3)$, $c = 20.358(3)$ Å, $\beta = 90.094(2)°$, $V = 3692$ Å^3. D_c ($Z = 4$) = 1.532 g cm^{-3}. $\mu_{Mo} = 6.6$ cm^{-1}; specimen: $0.30 \times 0.15 \times 0.10$ mm; 'T'$_{min/max} = 0.89$. $2\theta_{max} = 58°$; $N_t = 43278$, $N = 9393$ ($R_{int} = 0.032$), $N_o = 7121$; $R = 0.040$, $R_w = 0.049$.

Variata. The anion was modelled as rotationally disordered about the PF(1,2) line, F(3–6) modelled over two sets of sites, occupancies refining to 0.816(5) and complement. Disorder is also observed in the cation, the silver atom being modelled over two sets of sites, occupancies refining to 0.9081(7) and complement; no associated components of disorder in the ligand were resolvable.

$[Ag(\mathbf{5})]BF_4 \equiv C_{39}H_{42}AgBF_4N_4O_2$, $M = 793.5$. Triclinic, space group $P\bar{1}$ (C_i^1, No. 2), $a = 10.807(2)$, $b = 11.020(2)$, $c = 16.153(2)$ Å, $\alpha = 73.702(2)$, $\beta = 78.784(2)$, $\gamma = 72.043(2)°$, $V = 1744$ Å^3. D_c ($Z = 2$) = 1.511 g cm^{-3}. $\mu_{Mo} = 6.4$ cm^{-1}; specimen: $0.13 \times 0.10 \times 0.065$ mm; 'T'$_{min/max} = 0.87$. $2\theta_{max} = 53°$; $N_t = 16914$, $N = 7069$ ($R_{int} = 0.032$), $N_o = 5778$; $R = 0.042$, $R_w = 0.048$.

$[Ag(\mathbf{6})]PF_6\cdot CH_3CN \equiv C_{46}H_{48}AgF_6N_4O_2P\cdot CH_3CN$, $M = 982.8$. Monoclinic, space group $P2_1/c$, $a = 15.995(2)$, $b = 16.038(2)$, $c = 17.855(3)$ Å, $\beta = 95.680(2)°$, $V = 4558$ Å^3. D_c ($Z = 4$) = 1.432 g cm^{-3}. $\mu_{Mo} = 5.5$ cm^{-1}; specimen: $0.80 \times 0.22 \times 0.04$ mm; 'T'$_{min/max} = 0.87$. $2\theta_{max} = 58°$; $N_t = 53765$, $N = 11682$ ($R_{int} = 0.039$), $N_o = 8704$; $R = 0.039$, $R_w = 0.043$. $(x,y,z,U_{iso})_H$ (ligand) were refined.

$[Cu(\mathbf{6})(OH)]PF_6\cdot 2H_2O \equiv C_{46}H_{49}CuF_6N_4O_3P\cdot 2H_2O$, $M = 950.5$. Orthorhombic, space group $Pbca$ (D_{2h}^{15}, No. 61) $a = 16.347(4)$, $b = 20.768(5)$, $c = 24.865(6)$ Å, $V = 8442$ Å^3. D_c ($Z = 8$) = 1.496 g cm^{-3}. $\mu_{Mo} = 6.4$ cm^{-1}; specimen: $0.38 \times 0.32 \times 0.10$ mm; 'T'$_{min/max} = 0.81$. $2\theta_{max} = 50°$; $N_t = 55561$, $N = 7400$ ($R_{int} = 0.075$), $N_o = 5000$; $R = 0.068$, $R_w = 0.095$.

Variata. Difference map residues were modelled in terms of oxygen atoms, tentatively assigned as hydroxide (coordinated) or (lattice) water; associated hydrogen atoms were not resolved.

The following determinations were undertaken with the following general variations in procedure: the refinement was executed using SHELXL-97,[16] Gaussian absorption correction being applied in two instances, as indicated; reflection weights were $(\sigma^2(F_o^2) + AP^2 + BP)^{-1}$, $P = (F_o^2 + 2F_c^2)/3$ (A,B cited below). $R1(F)$, $wR2(F^2)$ are quoted.

$[Ni(\mathbf{2})(NO_3)_2]\cdot CH_3CN\cdot H_2O \equiv C_{34}H_{41}N_7NiO_9$, $M = 750.5$. Monoclinic, space group $P2_1/n$, $a = 18.416(4)$, $b = 8.693(2)$, $c = 23.139(5)$ Å, $\beta = 109.485(4)°$, $V = 3492$ Å^3. D_c ($Z = 4$) = 1.427 g cm^{-3}. $\mu_{Mo} = 6.2$ cm^{-1}; specimen: $0.33 \times 0.31 \times 0.22$ mm; $T_{min,max}$ (Gaussian correction) = 0.80, 0.89. $2\theta_{max} = 56.5°$; $N_t = 31495$, $N = 8234$ ($R_{int} = 0.025$), $N_o = 6797$; $R1(F) = 0.029$, $wR2(F^2) = 0.062$ ($A = 0.062$, $B = 0$).

$[Ni(\mathbf{3})](NO_3)_2\cdot H_2O \equiv C_{32}H_{38}N_6NiO_{10}$, $M = 709.4$. Monoclinic, space group $P2_1/n$, $a = 11.013(4)$, $b = 23.351(9)$, $c = 12.836(5)$ Å, $\beta = 91.737(12)°$, $V = 3300$ Å^3. D_c ($Z = 4$) = 1.424 g cm^{-3}. $\mu_{Mo} = 6.5$ cm^{-1}; specimen: $0.45 \times 0.42 \times 0.41$ mm; 'T'$_{min/max} = 0.90$. $2\theta_{max} = 56.6°$; $N_t = 32067$, $N = 7807$ ($R_{int} = 0.018$), $N_o = 7274$; $R1(F) = 0.074$, $R_w(F^2) = 0.019$ ($A = 0.005$, $B = 8$).

Variata. Difference map residues were modelled in terms of a disordered water molecule oxygen, associated hydrogen atoms not being located. The nitrate moieties also exhibit significant disorder, the components being modelled as rigid bodies.

$[Ni(\mathbf{5})](NO_3)_2\cdot 3CH_3OH \equiv C_{42}H_{54}N_6NiO_{11}$, $M = 877.6$. Triclinic, space group $P\bar{1}$, $a = 9.498(1)$, $b = 11.094(2)$, $c = 21.743(3)$ Å, $\alpha = 92.006(3)$, $\beta = 95.444(3)$, $\gamma = 111.507(3)°$, $V = 2116$ Å^3. D_c ($Z = 2$) = 1.378 g cm^{-3}. $\mu_{Mo} = 5.3$ cm^{-1}; specimen: $0.38 \times 0.14 \times 0.11$ mm; $T_{min,max}$ (Gaussian correction) = 0.84, 0.95. $2\theta_{max} = 56.7°$; $N_t = 21470$, $N = 9931$ ($R_{int} = 0.034$), $N_o = 8015$; $R1(F) = 0.035$, $wR2(F^2) = 0.080$ ($A = 0.03$, $B = 0$).

Computational study

The DFT computations were performed with the Amsterdam Density Functional 1999.02 (ADF)[17] program package on a Silicon Graphics Origin 2000 computer (56 MIPS R10000 64-Bit CPU with 195 MHz and 17 GB Memory). All structures were optimised without imposing symmetry constraints. The molecular orbitals were expanded in an uncontracted set of Slater-type orbitals (STO's) containing diffuse functions. The basis is of triple-zeta quality, augmented with one or two polarisation functions. The cores were treated by the frozen-core approximation.[18] The numerical integration was performed using the procedure developed by Baerends *et al.*[19] The Becke–Perdew (BP86) functional was used for the calculations, this uses Becke's[20] gradient correction for the local expression of the exchange energy and Perdew's[21] gradient correction for the local expression of the correlation energy. The convergence criteria for the geometry optimisations, which use analytical derivatives,[22] were set to 1×10^{-3} hartree for the changes in energy, 1×10^{-3} hartree Å^{-1} for the energy gradient, 1×10^{-3} Å for the changes between old and new bond lengths, and 0.3° for changes in bond and dihedral angles. All stationary points on the hypersurface were characterised as true minima by frequency analysis.

Syntheses

The syntheses of **1**[10,23] have been described previously.

Cobalt(II), nickel(II), zinc(II), and cadmium(II) nitrate complexes of 2. The required hydrated metal(II) nitrate in methanol (1.31 mL, 0.200 M) was added to a solution of **2** in methanol (3.00 mL, 0.0872 M). The respective solutions were filtered and crystallisation of the corresponding metal complexes were induced by diffusion of diethyl ether vapour into each solution. In each case, the product was removed by filtration and dried under vacuum over phosphorus pentoxide. In most instances, in separate experiments, crystals suitable for X-ray crystallography were grown by slow diffusion of diethyl ether vapour into a methanol or acetonitrile solution of the respective complexes.

[Co(2)(NO$_3$)$_2$]·0.5CH$_3$OH·0.5H$_2$O. Yield 52% [Found $(CoLNO_3)^+$, m/z 629.1 (ES) $C_{32}H_{36}CoN_5O_5$ requires 629.2] (Found: C, 54.2; H, 5.4; N, 11.8. Calc. for $C_{32}H_{36}CoN_6O_8\cdot 0.5CH_3OH\cdot 0.5H_2O$: C, 54.47; H, 5.49; N, 11.73%).

[Ni(2)(NO$_3$)$_2$]·CH$_3$OH·3H$_2$O. Yield 62% [Found $(NiL - H)^+$, m/z 565.3 (ES) $C_{32}H_{35}N_4NiO_2$ requires 565.2] (Found: C, 51.2; H, 6.1; N, 10.8. Calc. for $C_{32}H_{36}N_6NiO_8\cdot CH_3OH\cdot 3H_2O$: C, 50.98; H, 5.96; N, 10.81%).

[Zn(2)(NO$_3$)$_2$]·1.5CH$_3$OH·2.5H$_2$O. Yield 43% [Found $(ZnL - H)^+$, m/z 571.3 (ES) $C_{32}H_{35}N_4O_2Zn$ requires 571.2]

Table 1 Physical properties of the complexes of **2**–**6**

Complex	Colour	Λ^a	μ^b/μ_B	Electronic spectra [c]/nm (ε/M^{-1} cm^{-1})
[Co(**2**)$(NO_3)_2$]·0.5CH_3OH·0.5H_2O	Pink	75	4.59	470 (sh), 500 (ε = 34), 545 (sh)
[Ni(**2**)$(NO_3)_2$]·CH_3OH·3H_2O	Pale blue	86	3.37	380 (ε = 35), 610 (ε = 22), 995 (ε = 24)
[Zn(**2**)$(NO_3)_2$]·1.5CH_3OH·2.5H_2O	Pale blue	83		
[Ag(**2**)]BF_4	Colourless	91		
[Cd(**2**) $(NO_3)_2$]·CH_3OH·0.5H_2O	Colourless	110		
[Ni(**3**)]$(NO_3)_2$·2.5H_2O	Pale blue	119	3.17	560 (ε = 35), 790 (ε = 27), 825 (ε = 32), 1200 (ε = 11)
[Ag(**4**)]PF_6	Colourless	96		
[Ni(**5**)]$(NO_3)_2$·H_2O	Pale blue	111	3.36	575 (ε = 15), 780 (ε = 26), 830 (ε = 27), 1290 (ε = 12)
[Ag(**5**)]BF_4	Colourless	93		
[Cu(**6**)OH]PF_6·0.5H_2O	Violet	89		515 (ε = 194), 645 (ε = 193)
[Ag(**6**)]PF_6	Colourless	89		

[a] Conductance (S cm^2 mol^{-1}) at 25 °C in methanol; expected range for a 1 : 1 electrolyte in methanol is 80–115 S cm^2 mol^{-1} while that for a 2 : 1 electrolyte is 160–220 S cm^2 mol^{-1} see ref. 24. [b] Magnetic moment at 25 °C. [c] In methanol.

(Found: C, 50.7 H, 5.8; N, 10.7. Calc. for $C_{32}H_{36}N_6O_8Zn$·1.5CH_3OH·2.5H_2O: C, 50.86 H, 5.99; N, 10.62%).

[Cd(2)$(NO_3)_2$]·CH_3OH·0.5H_2O. Yield 47% [Found (CdL − H)$^+$, *m*/*z* 621.2 (ES) $C_{32}H_{35}CdN_4O_2$ requires 621.2] (Found: C, 50.3; H, 5.0; N, 10.5. Calc. for $C_{32}H_{36}CdN_6O_8$·CH_3OH·0.5H_2O: C, 50.42; H, 5.26; N, 10.69%).

Silver(I) tetrafluoroborate complexes of 2 and 5. Silver(I) tetrafluoroborate (51 mg, 0.26 mmol) in methanol (2 mL) was added to a solution of the respective ligand in methanol (3.00 mL, 0.26 mmol). The solution was filtered and crystallisation of the metal complex was induced by diffusion of diethyl ether vapour into the reaction solution. The product was removed by filtration and dried under vacuum over phosphorus pentoxide. Crystals suitable for X-ray crystallography were grown by slow diffusion of diethyl ether into a methanol solution of the respective complexes.

[Ag(2)]BF_4. Yield 41% [Found (AgL)$^+$, *m*/*z* 615.2 (ES) $C_{32}H_{36}AgN_4O_2$ requires 615.2] (Found: C, 54.7; H, 5.4; N, 7.9. Calc. for $C_{32}H_{36}AgBF_4N_4O_2$: C, 54.65; H, 5.16; N, 7.97%).

[Ag(5)]BF_4. Yield 47% [Found (AgL)$^+$, *m*/*z* 705.2 (ES) $C_{39}H_{42}AgN_4O_2$ requires 705.2] (Found: C, 59.0; H, 5.4; N, 7.1. Calc. for $C_{39}H_{42}AgBF_4N_4O_2$: C, 59.04; H, 5.38; N, 7.12%).

Nickel(II) nitrate complexes of 3 and 5. These compounds were obtained by an analogous procedure to that described above for the corresponding complex of **2**. Crystals suitable for X-ray crystallography were grown by slow diffusion of diethyl ether into a methanol solution of the respective complexes.

[Ni(3)]$(NO_3)_2$·2.5H_2O. Yield 47% [Found (NiL − H)$^+$, *m*/*z* 565.3 (ES) $C_{32}H_{35}N_4NiO_2$ requires 565.2] (Found: C, 52.4; H, 5.4; N, 11.5. Calc. for $C_{32}H_{36}NiN_6O_8$·2.5H_2O: C, 52.19; H, 5.61; N, 11.41%).

[Ni(5)]$(NO_3)_2$·H_2O. Yield 52% [Found (NiLNO$_3$)$^+$, *m*/*z* 718.1 (ES) $C_{39}H_{42}N_5NiO_5$ requires 718.3] (Found: C, 58.3; H, 5.5; N, 10.4. Calc. for $C_{39}H_{42}N_6NiO_8$·H_2O: C, 58.59; H, 5.55; N, 10.51%).

Silver(I) hexafluorophosphate complexes of 4 and 6. Silver(I) hexafluorophosphate (25 mg, 0.10 mmol) in acetonitrile (2 mL) was added to **4** in methanol or **6** in 1 : 1 acetonitrile : chloroform (4 mL, 0.10 mmol). The solution was filtered and crystallisation of the metal complex was induced by diffusion of diethyl ether vapour into the filtrate. The product was removed by filtration and dried under vacuum over phosphorus pentoxide. Crystals suitable for X-ray crystallography were grown by slow diffusion of diethyl ether into an acetonitrile solution of the respective complexes.

[Ag(4)]PF_6. Yield 64% [Found (AgL)$^+$, *m*/*z* 705.3 (ES) $C_{39}H_{42}AgN_4O_2$ requires 705.2] (Found: C, 54.7; H, 5.4; N, 7.9. Calc. for $C_{32}H_{36}AgBF_4N_4O_2$: C, 54.65; H, 5.16; N, 7.97%).

[Ag(6)]PF_6. Yield 54% [Found (AgL)$^+$, *m*/*z* 795.4 (ES) $C_{46}H_{48}AgN_4O_2$ requires 795.3] (Found: C, 58.7; H, 5.1; N, 6.1. Calc. for $C_{46}H_{48}AgBF_4N_4O_2$: C, 58.67; H, 5.14; N, 5.95T%).

[Cu(6)OH]PF_6·0.5H_2O. Copper(I) hexafluorophosphate in acetonitrile (2.96 mL, 0.05 M) was added to a solution of **6** in acetonitrile (10.0 mL, 0.015 M). The solution was filtered and crystallisation of the metal complex was induced by slow evaporation of the solution. Recrystallisation from aqueous ethanol yielded the pure product as fine violet needles. The product was removed by filtration and dried under vacuum over phosphorus pentoxide. Yield 0.027 g, 14% [Found (CuL)$^{2+}$, *m*/*z* 345.3 (ES) ($C_{46}H_{48}CuN_4O_2$)/2 requires 345.2] (Found: C, 59.7; H, 5.3; N, 6.1. Calc. for $C_{46}H_{48}CuF_6N_4O_2P$·5H_2O: C, 59.83; H, 5.46; N, 6.07%). Crystals suitable for X-ray crystallography were grown by slow evaporation of a solution of the complex in acetonitrile.

An attempt to synthesise the silver(I) hexafluorophosphate complex of **2** yielded an X-ray quality crystal whose X-ray structure indicates that hydrolysis of hexafluorophosphate has occurred; with the product being of type [(**2**)H_2](PF_6)-(PF_2O_2)·H_2O·CH_3CN incorporating a doubly protonated ligand together with PF_2O_2 and PF_6 anions.

Results and discussion

Metal complexes

In an attempt to obtain crystalline products suitable for X-ray diffraction studies, solid metal complexes of **2**–**6** with cobalt(II), nickel(II), copper(II), zinc(II), cadmium(II) and silver(I) was isolated and characterised (Table 1). The conductance values in methanol (Table 1) for all the complexes approximate those expected for a 1 : 1 electrolyte thus indicating that the silver(I) complexes are essentially completely ionised under the conditions employed, while the cobalt(II), nickel(II), copper(II), zinc(II) and cadmium(II) complexes retain one bound anion in this solvent.[24]

The magnetic moments (Table 1) of the pink cobalt complex of **2** and the blue nickel complexes of **2**, **3** and **5** confirm their high spin nature. The visible spectra in methanol are consistent with these complexes having distorted octahedral coordination geometries.[25]

The visible spectrum of the copper complex [Cu(**6**)OH]-PF_6·2H_2O showed a broad envelope of bands in the 450–750 nm region with maxima occurring at 516 and 644 nm respectively. The shape of the observed EPR signal at liquid nitrogen temperature (DMF glass) suggests the presence of two copper species under the conditions employed, each with the metal in an axially symmetrical environment elongated

Table 2 Ligand protonation constants and metal stability constants for **1**, **2**, **5** and **6** [a]

Ligand	Log K_H			Log K_{ML} [b]						
	K_1	K_2	K_3	Co^{2+}	Ni^{2+}	Zn^{2+}	Cd^{2+}	Cu^{2+}	Ag^{+}	Pb^{2+}
1	9.86	8.58	—	9.2	~10	9.4	9.5	>14	>13	9.8
2	10.26	7.55	—	-[c]	—	7.8	8.4	>14	>14	7.5
5	9.64	6.14	—	-[c]	4.7	-[c]	6.1	12.5	10.2	5.5
6	8.95	5.97	—	<4	-[c]	<4	<4	-[c]	>8	<4

[a] In 95% methanol; I = 0.1 M, $(C_2H_5)_4NClO_4$, 25 °C; unless otherwise noted ligand protonation constants (log K_1 and log K_2) are ±0.05 while log K values for complex formation are ±0.1; ligand **4** proved to be of too low solubility for study. [b] Each value is the mean of at least two (and up to five) determinations at different metal : ligand ratios rounded to the first decimal place; data for **1** taken from ref. 23. [c] Precipitation, slow approach to equilibrium or competing hydrolysis inhibited log K determination in this case.

along the z-axis (as $g_{\|} > g_{\perp}$). Two $g_{\|}$ values could be assigned (2.204 and 2.154); however, only one $g_{\perp}$ value could be discerned, 2.082, reflecting the complex nature of the spectrum. No superhyperfine splitting due to coupling to ^{14}N nuclei was observed. While the two species perhaps arise from the presence of 'frozen' conformers, in the absence of further evidence it appears inappropriate to speculate further concerning this.

Potentiometric titrations

The protonation constants for the respective macrocycles were obtained by potentiometric (pH) titration in 95% methanol (I = 0.1 M, $N(C_2H_5)_4ClO_4$) and are listed in Table 2. As in previous studies, this solvent mixture was employed to overcome the generally restricted solubility of ligands of the present type (and/or their metal complexes) in water. Where possible, log K values corresponding to the formation of 1 : 1 (metal : ligand) species were obtained in each case by analysis of the initial portions of the respective titration curves. The log K data for **2**, **5** and **6** are summarised in Table 2 and, for comparison, stability data for the parent mixed-donor system **1**[23] is also included. The general trend of a decrease in the pK_a values on progressive N-benzylation follows previously observed trends.[5]

Unfortunately, owing to precipitation and/or competing hydrolysis, it was only possible to obtain log K values for a selection of the 1 : 1 complexes of the seven metals investigated with **2**, **5** and **6** (see Table 2). Nevertheless, a comparison of the values that were obtained with those for the unsubstituted parent ring, **1** indicates that, in general, selectivity for copper(II) and silver(I) appears to be maintained as the degree of N-benzylation is increased along **2**–**6**. While the situation is not clear cut, overall the results are not inconsistent with 'selective detuning' taking place,[5] especially when the relative log K values for the respective ligand complexes of the remaining five metals are compared.

Liquid–liquid extraction studies

Liquid–liquid extraction experiments (water/chloroform) using the radiotracer technique employing the isotopes ^{110m}Ag, ^{65}Zn, ^{60}Co and ^{64}Cu and **1**–**6** have been carried out. The chloroform phase consisted of a solution of the macrocycle (1.0×10^{-3} M) while the aqueous phase contained the metal (1.0×10^{-4} M) and picric acid (5.0×10^{-3} M). This phase was buffered at pH 6.2 with MES/NaOH buffer. The initial experiments involved the extraction of silver(I) under these conditions and extraction values of between 85 and 95% were obtained for all systems (Fig. 1). That is, **1**–**6** are all excellent extractants for this ion under the conditions employed.

For comparison, extractions in the absence of picrate ion but in the presence of a corresponding concentration of sodium nitrate (5.0×10^{-3} M), employing the same buffer system, were carried out (Fig. 1). Surprisingly, the extraction efficiency using the partial benzylated systems **2**–**5** is comparable in the presence of either nitrate or picrate. This result is in contrast to most metal extraction systems with organic ligands[26] showing the anion influence on metal extraction follows the lipophilicity

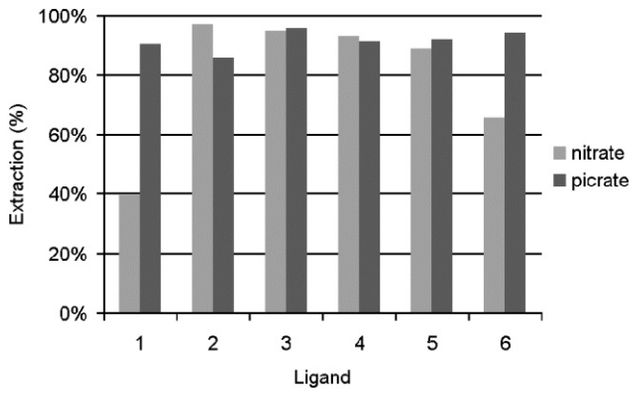

Fig. 1 Silver(I) extraction (water/chloroform) by ligands **1**–**6** with picrate or nitrate as the anion at pH 6.2 (MES/NaOH buffer) and 26 ± 2 °C; [L] = 1×10^{-3} M.

order of Hofmeister.[27] This unexpected effect of the nitrate counter ion on the silver extraction could reflect either coordination of the nitrate direct to the silver ion or its binding to a (secondary) amino hydrogen site on the ligand. The first situation was observed for the nitrate complexes of **2** with cobalt(II), nickel(II), zinc(II) and cadmium(II) (see Figs. 7 and 9) in the solid state, while the second corresponds to the situation in the solid copper(II) nitrate complex of **1**.[23] Similar possible binding patterns for the extraction system leading to increased silver extraction has also been discussed for amino cryptands[28] and the silver complex of an azathia-macrocycle incorporating an urea side arm.[29] In the case of ligand **1**, the extraction of silver(I) in the presence of nitrate is clearly lower than when picrate anion is present. This most likely reflects the lower lipophilicity of this unsubstituted ligand leading to protonated ligand and/or complex bleeding into the aqueous phase. For the interpretation of the extraction results it is interesting to note that for the lipophilic tribenzylated ligand, **6**, extraction of silver(I) in the presence of nitrate is also lower than when picrate is present. The latter presumably reflects the lack of secondary amines in the structure of **6** in comparison with **2**–**5** leading to the inhibition of (hydrogen bond) association of this ligand with the nitrate anion in the organic phase — thus favouring the observed high silver extraction with ligands **2**–**5** in the presence of nitrate.

In an attempt to determine the stoichiometry of the extracted species, extraction experiments were performed in which the concentration of the ligand was varied while the metal ion concentration was maintained at 1×10^{-4} M and the anion concentration was effectively constant. The log D_M (= $[M^{n+}]_{org}/[M^{n+}]_{aq}$) was then plotted against the log of the macrocycle concentration and, provided a 'simple' equilibrium is involved, the slope of this plot gives the stoichiometry of the extracted species directly. Thus:

$$M^{n+}_{(aq)} + nA^{-}_{(aq)} + sL_{(org)} \rightleftharpoons ML_sA_{n(org)} \quad (1)$$

$$K_{Ex} = \frac{[ML_sA_n]_{(org)}}{[M^{n+}]_{(aq)}\,[L]^{s}_{(org)}\,[A^{-}]^{n}_{(aq)}} \quad (2)$$

$$\log D_M = \log K_{Ex} + n \log[A^-]_{(aq)} + s \log[L]_{(org)} \quad (3)$$

For ligand **4** (and silver nitrate) variable ligand concentration experiments were carried out at two different pH values (Fig. 2). The gradient in both cases approximated one, reflecting the expected 1 : 1 (ligand to metal) complex stoichiometry for this system in solution. Ligand **1** was also used for a range of similar extraction experiments with cobalt(II), zinc(II), copper(II), and silver(I) in the presence of nitrate and picrate, but unfortunately, the results indicated that bleeding of the respective complexes into the aqueous layer occurred for this less lipophilic ligand system.

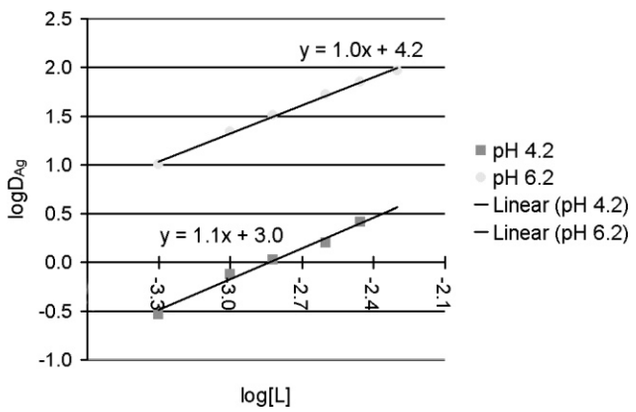

Fig. 2 Variable ligand concentration experiments for **4** with silver(I) and nitrate as the anion at pH 4.2 (citric acid/NaOH buffer) and pH. 6.2 ± 0.1 (MES/NaOH buffer), 26 ± 2 °C.

A comparison of the percent extraction for each of the ligands **1**–**6** for the three metals cobalt(II), zinc(II), and silver(I), with picrate as the anion (MES/NaOH buffer, pH 6.2 ± 0.1,) is given in Fig. 3. High extraction efficiencies for silver(I) remain effectively little changed on progressive *N*-benzylation along this ligand series, whereas for cobalt(II) and zinc(II), with the possible exception of the system incorporating **1**, the percent extraction was minimal (or zero) in all cases for **1**.

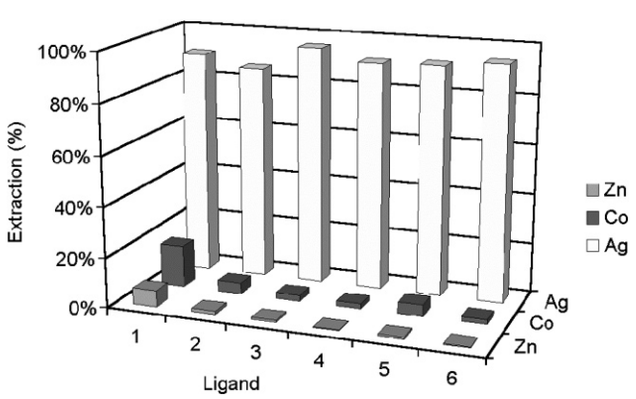

Fig. 3 Percent cobalt(II), zinc(II), and silver(I) extraction by ligands **1**–**6** with picrate as the anion at pH. 6.2 (MES/NaOH buffer) and 26 ± 2 °C.

A comparison of the extraction behaviour of copper(II) by **1** and **6** against that for silver(I) is shown in Fig. 4. While extraction of silver(I) remains high for the tri-*N*-benzyl derivative **6**, the degree of extraction decreases significantly for copper(II) for this ligand. That is, overall, the latter system yields considerably enhanced extraction discrimination for silver over copper relative to its parent (unsubstituted) ring. Combining this result with the results for cobalt and zinc (Fig. 3) indicates that, overall, **6** gives rise to excellent discrimination for silver over each of the other metal ions investigated.

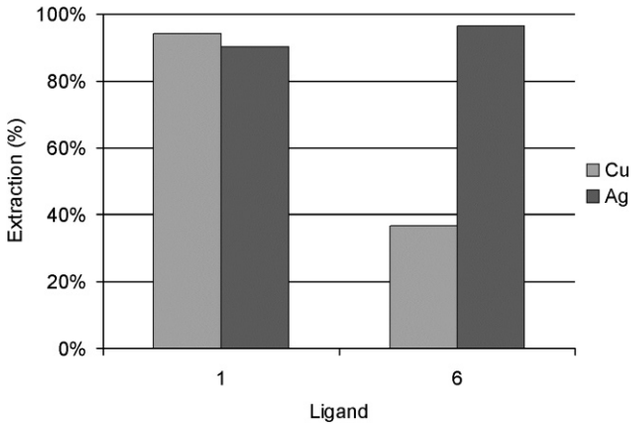

Fig. 4 Percent copper(II) and silver(I) extraction by **1** and **6** with picrate as the anion at pH 6.2 (MES/NaOH buffer) and 26 ± 2 °C.

Membrane transport

In addition to the single ion extraction studies competitive mixed metal transport experiments (water/chloroform/water) have been undertaken for which the chloroform membrane phase contained the ionophore, chosen from **1**–**6** respectively, at 1×10^{-3} M. The aqueous source phase contained equimolar concentrations of the nitrate salts of cobalt(II), nickel(II), copper(II), zinc(II), cadmium(II), silver(I) and lead(II), with individual metal ion concentrations being 1.0×10^{-2} M. Transport was performed against a back gradient of protons with palmitic acid (4×10^{-3} M) also present in the organic phase. A main role of the latter is to aid the transport process by providing a lipophilic counterion in the organic phase (after proton loss to the aqueous source phase) for charge neutralisation of the metal cation being transported.

Transport flux values for both copper(II) and silver(I) for each of **1**–**6** are illustrated in Fig. 5. The values for cobalt(II), nickel(II), zinc(II), cadmium(II) and lead(II) were all less than 20×10^{-7} mol (24 h)$^{-1}$ indicating negligible transport under the present conditions (values are within experimental error of zero).[30] Clearly, the parent ligand **1** is a poor ionophore for all seven metals (although marginal transport of copper(II) was detected), a fact that is again probably related to its lower lipophilicity arising from the absence of *N*-benzyl substituents. In accord with this, the singly benzylated species **2** and **3** yielded enhanced transport of copper(II) but now silver(I) transport is observed as well. Moving to the di-*N*-benzylated derivatives **4** and **5** these both show enhanced selectivity and efficiency for silver(I) transport. Within the limits of accuracy of the experiments, sole selectivity for silver was attained in the case of **4**, with **5** yielding similar behaviour towards silver(I) but with a minor amount of copper(II) also being transported in this case. The final ionophore, **6**, in which all three ring nitrogens are benzylated, also yielded sole transport selectivity for silver(I), although the efficiency of transport was somewhat less in this case relative to that observed for **4** and **5**. Under the present conditions, the di- and tri-benzylated ligands **4**–**6** each show marked selectivity for silver over the remaining six metal ions present in the aqueous phase. As before, this result is in general accord with these ligand systems inducing discrimination for silver *via* a 'selective detuning' mechanism.

X-Ray structures

Single crystal 'low'-temperature X-ray structure determinations have been carried out for a salt of the ligand **2**, three of its divalent metal nitrate complexes and a silver(I) tetrafluoroborate complex. In all cases, one formula unit devoid of crystallographic symmetry comprises the asymmetric unit of the structure, the stoichiometries and connectivities being consistent with the formulations given above; the three divalent metal complexes, $[M(\mathbf{2})(NO_3)_2]$·methanol solvate (M = Co,

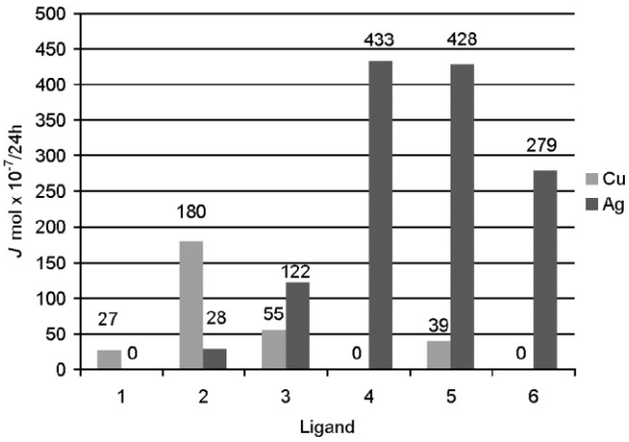

Fig. 5 The copper(II) and silver(I) transport fluxes for the six ligands **1**–**6** in the chloroform membrane transport experiment.

Zn, Cd), are isomorphous. The protonated ligand, $[(\mathbf{2})H_2]^{2+}$, adopts a conformation that is close to *m* symmetry (Fig. 6); in the metal complexes this is followed closely except in the bonds to either side of the central nitrogen which differ, breaking that symmetry.

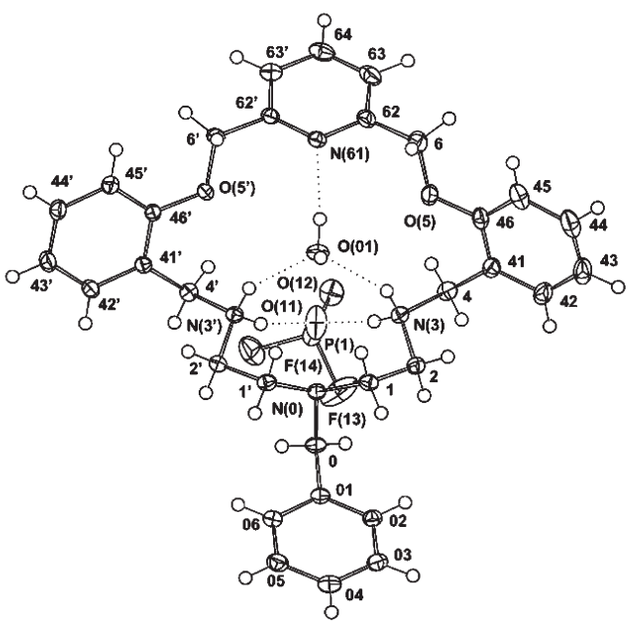

Fig. 6 Projection of the $[(\mathbf{2})H_2(H_2O)(PF_2O_2)]^+$ aggregate.

The formulation of the ligand salt is adventitious, complex and interesting (Fig. 6). Hydrogen atom refinement establishes the cation to be doubly protonated, $[(\mathbf{2})H_2]^{2+}$. Charge balance is achieved *via* one hexafluorophosphate anion, slightly disordered, and a second counterion, modelled plausibly in the refinement as $F_2O_2^-$, a commonly occurring hexafluorophosphate hydrolysis product. The latter, together with a water molecule make up a cationic cluster (Fig. 6), $[(\mathbf{2})H_2(H_2O)(PF_2O_2)]^+$, the final component an acetonitrile molecule, devoid of close interactions. The structure of the cluster is interesting, the oxygen of the water molecule 'chelated' by a pair of protonated N(3,3′) amine hydrogen atoms O(01)···H(3a,3b′) 2.19(2), 2.11(2) Å, while unprotonated N(61) interacts with a water hydrogen, N(61)···H(01a) 2.02(3) Å, a motif that also occurs in the solvating methanol/water interactions of the set of divalent metal complexes incorporating **2** (see Fig. 7). The other pair of protonated amine hydrogen atoms chelates one of the anionic oxygen atoms: O(11)···H(3b,3a′) 1.91(2), 1.97(2) Å. The other water molecule hydrogen interacts with the other (symmetry related) anionic oxygen O(12)···H(O1b) (x, ½ − y, ½ + z) 1.99(2) Å, linking the clusters into strings.

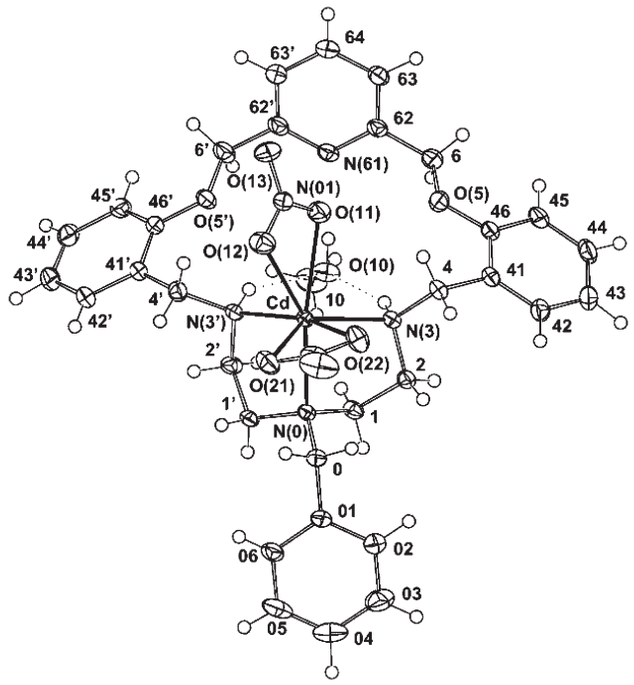

Fig. 7 Projection of the $[Cd(\mathbf{2})(NO_3)_2]$ molecule (as broadly representative of the cobalt(II) and zinc(II) species also).

In the cobalt(II), zinc(II) and cadmium(II) complexes of **2**, the metal supplants the anion oxygen atom in respect of its interactions with the deprotonated chelating amines, the local symmetry about N(0) distorting so that the pair of five-membered metallacycle rings are quasi-2, rather than quasi-*m*, in their relationship. The coordination sphere about the metal comprises this pair of nitrogen atoms and N(0) between them, as a tridentate, with a pair of chelating nitrate groups. The latter vary in their interactions with the metal, nitrate 2 essentially symmetrically chelating, while nitrate 1 is unsymmetrically chelating, the more so as the metal size diminishes (Table 3). The differences in the nature of the associated oxygens are reflected in the distances and angles about the central nitrogen atoms. In the copper(II) complex of **6** (Fig. 8), wherein the effective coordination number and geometry are driven toward planar four-coordinate by the electron configuration, the ligand (indeed the cation) conformation becomes quasi-*m* once more, but with a different disposition consequent upon the N_3-donors of the pair of metallacycles becoming *mer* rather than *fac* in the coordination sphere. Four-coordinate copper complexes that partner a hydroxo ligand with three coordinating nitrogen atoms are rare, with only two being listed on the current release of the Cambridge Structural Database.[31]

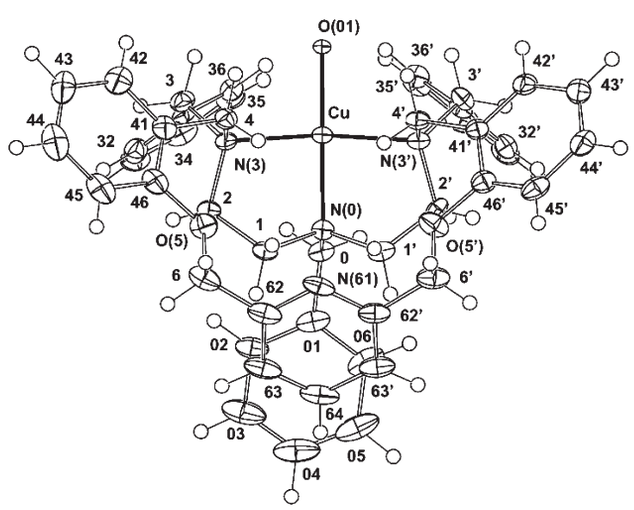

Fig. 8 Projection of the $[Cu(\mathbf{6})(OH)]^+$ cation, projected normal to the coordination plane.

Table 3 Metal atom environments, [M(**2**)$(NO_3)_2$]; *r* is the metal–donor atom distance (Å), the other entries being the angles (degrees) subtended by the relevant atoms at the head of the row and column. The four values in each entry are for M = Co, Zn, Cd, Ni respectively

Atom	*r*	N(3)	N(3′)	O(11)	O(12)	O(21)	O(22)
N(0)	2.215(2)	81.43(7)	81.70(6)	141.32(6)	166.88(7)	88.88(7)	97.45(6)
	2.221(3)	83.0(1)	82.8(1)	143.7(1)	166.3(1)	89.7(1)	94.7(1)
	2.412(2)	77.17(5)	77.16(5)	146.09(5)	154.01(5)	88.59(5)	99.13(5)
	2.122(1)	84.69(5)	84.65(5)	152.13(4)	166.84(4)	92.22(4)	98.83(4)
N(3)	2.106(2)		105.93(6)	74.49(6)	111.62(7)	145.62(6)	90.81(6)
	2.086(3)		108.0(1)	74.5(1)	110.3(1)	144.7(1)	90.3(1)
	2.302(1)		107.15(5)	80.20(5)	128.64(6)	134.70(5)	87.23(5)
	2.079(1)		106.46(4)	118.94(4)	86.87(4)	156.59(4)	96.35(4)
N(3′)	2.117(2)			76.52(6)	95.46(6)	105.15(6)	162.84(6)
	2.103(3)			77.6(1)	95.7(1)	105.3(1)	161.0(1)
	2.308(1)			85.89(5)	90.18(5)	111.19(5)	163.63(5)
	2.068(1)			100.84(4)	88.08(5)	96.32(4)	157.16(4)
O(11)	2.863(2)				48.61(6)	127.42(6)	112.49(6)
	2.905(4)				47.8(1)	124.8(1)	113.3(1)
	2.526(2)				52.59(5)	125.11(5)	104.67(5)
	3.289(1)				40.47(3)	60.13(4)	66.02(3)
O(12)	2.057(2)					79.46(7)	81.47(6)
	2.072(3)					77.5(1)	82.3(1)
	2.343(2)					74.80(6)	86.62(5)
	2.077(1)					99.49(4)	92.12(4)
O(21)	2.179(2)						57.70(5)
	2.232(3)						55.8(1)
	2.478(2)						52.51(5)
	2.118(1)						61.12(3)
O(22)	2.263(2)						
	2.367(3)						
	2.400(1)						
	2.129(1)						

The structure of the nickel(II) counterpart of **2** has also been determined (Fig. 9). With a different solvate complement, this complex is not isomorphous with its cobalt(II), zinc(II) and cadmium(II) analogues, presumably as a consequence of the effective nickel atom radius being smaller than that of the other metal atoms (Table 3). Although the relative dispositions of the components of the molecule are qualitatively similar to those of the other arrays (Fig. 7), the differences are significant and substantial, chiefly arising from changes in the disposition of nitrate 1 which is now clearly unidentate with Ni–O(11) being very long at 3.289(1) Å. (In the atom numbering O(12) defines the shorter of the pair of Ni–O bonds from this nitrate; however, a more appropriate perception is that, in terms of the Co, Zn and Cd numbering, the longer and shorter of the two bonds have interchanged their roles, rather than the nitrate group having rotated about the N–O(13) (uncoordinated) bond by *ca.* 180°.)

With the silver(I) complexes (Figs. 10–13), a wide diversity of forms is found; in each case, one formula unit comprises the asymmetric unit, the $[AgL]^+$ (L = **2**, **4**–**6**) cations devoid of symmetry and showing close interactions with other species. Given the predominance of nitrogen donors, some tendency toward linear N–Ag–N arrays would not be surprising. Although all silver complexes have coordination numbers greater than two, such a tendency towards linear coordination is nonetheless

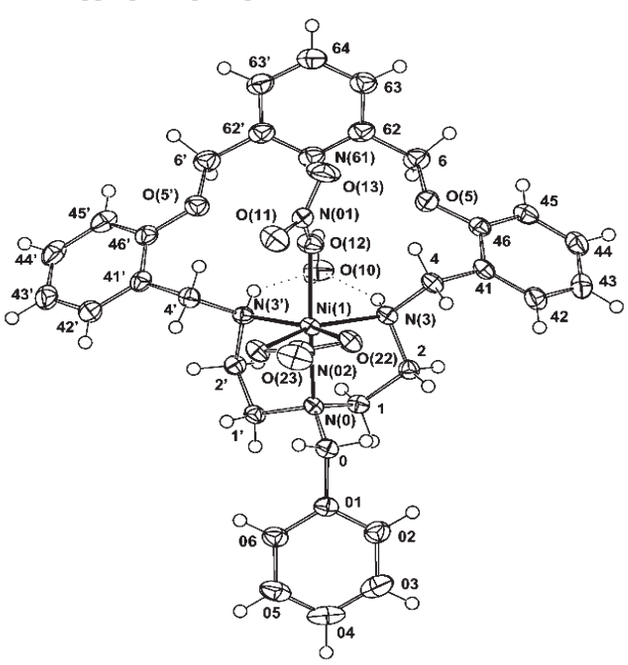

Fig. 9 Projection of the [Ni(**2**)$(NO_3)_2$] molecule showing the modification of the coordination of nitrate 1 to become unidentate, and the replacement of the hydrogen bonded methanol solvent molecule by water.

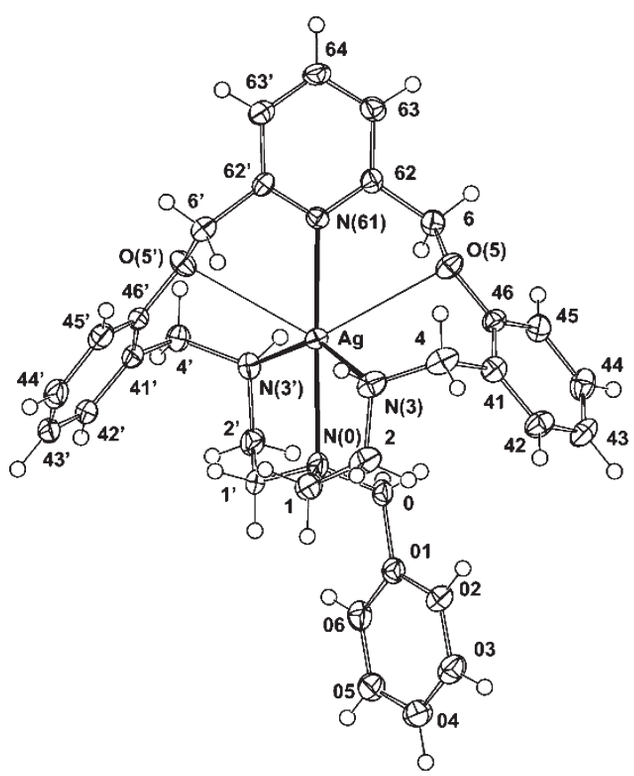

Fig. 10 Proection of the $[Ag(2)]^+$ cation.

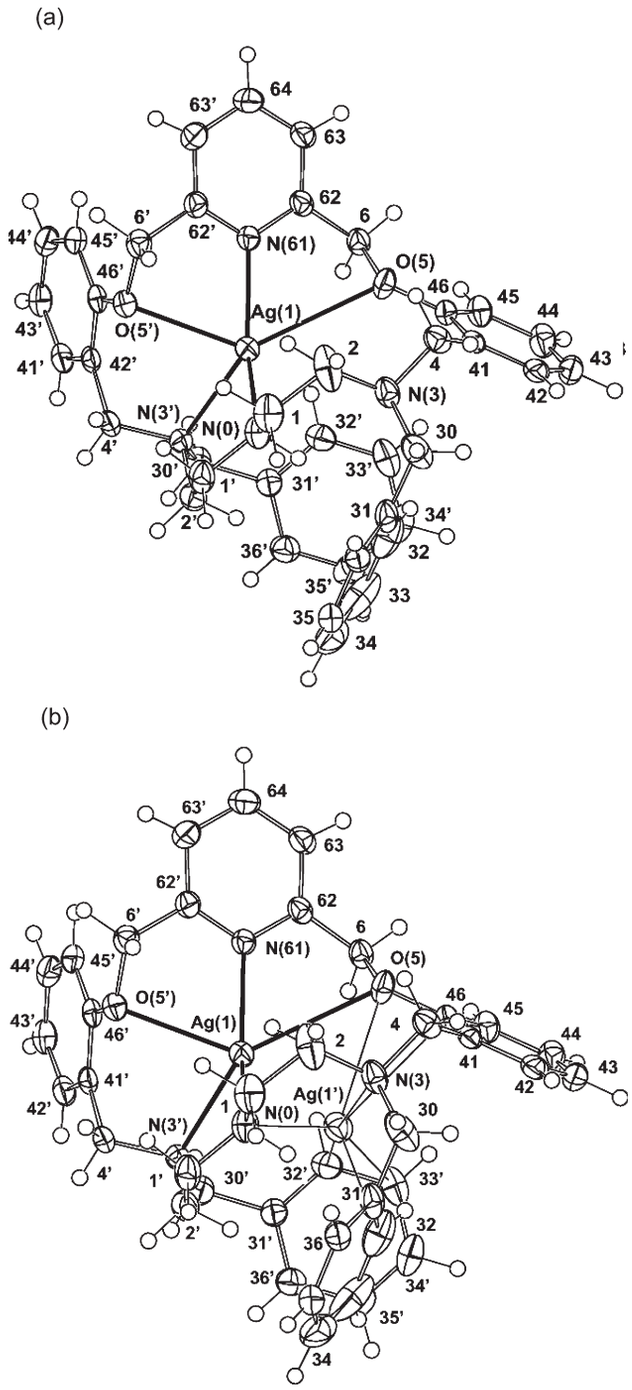

Fig. 11 (a, b) Projections of the major and minor components of the $[Ag(\mathbf{4})]^+$ cation.

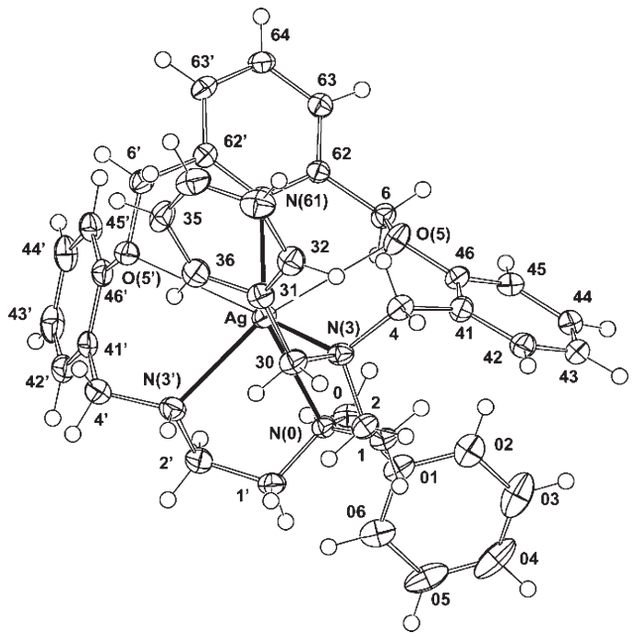

Fig. 12 Projection of the $[Ag(\mathbf{5})]^+$ cation.

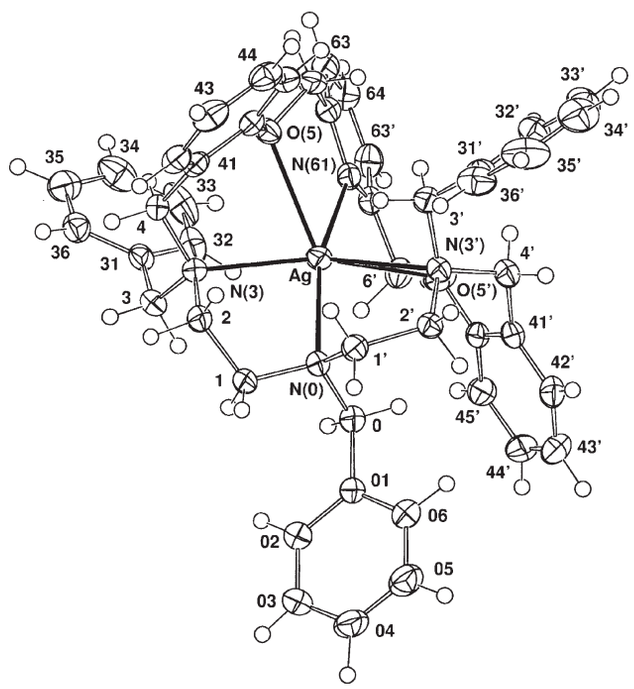

Fig. 13 Projection of the $[Ag(\mathbf{6})]^{2+}$ cation.

suggested by the observation that in $[Ag(\mathbf{2})]^+$ (Fig. 10), the N(0)–Ag–N(61) angle is 176.5(1)° and in the $[Ag(\mathbf{6})]^+$ the angle is 160.53(8)° (Fig. 13); the shortest Ag–N distance among these is 2.353(2) Å. With coordination numbers effectively greater than two, the N(3)N(0)N(3′) triad might be expected to form an effective tridentate. In $[Ag(\mathbf{2})]^+$ this might be considered to be the case (Fig. 10), with the N(3)–Ag–N(3′) angle being the largest among the four $[AgL]^+$ cations, but still only 147.0(1)° (see Table 4). In $[Ag(\mathbf{4})]^+$, N(3) is well removed from the silver atom and the above motif is effectively non-existent (Fig. 11). The effects of the pendant groups on the macrocycle conformation also are diverse, and, one suspects, predominantly indirect by way of crystal packing effects. Parallel approaches of aromatic planes are seen to be widespread. Of particular interest is the disorder observed in $[Ag(\mathbf{4})]^+$ where an alternative Ag^+ site at 10% occupancy is identified, well removed from the main component. In this component the pendant ring C(3*n*) is located in such a manner that Ag′···ring contacts, suggestive of the familiar Ag/aromatic ring interactions, are observed [Fig. 11(b)]; while such behaviour for the silver complexes is not widespread, contacts of this type could, of course, be of greater significance in solution.

Similar nickel environments occur in the nickel(II) complexes of **3** (Fig. 14) and **5** (Fig. 15), with the ligands in both cases behaving as sexadentates with similar conformations, presumably in response to a more stringent quasi-octahedral coordination imperative for this metal ion.

Clear-cut strong interactions in the crystal packings of the metal complexes are relatively limited. Well-defined contacts from the coordinated anions to the hydroxylic solvent molecules are observed in the cobalt(II), zinc(II), cadmium(II) and nickel(II) complexes of **2** (Table 5), NH(3,3′) also 'chelating'. In the copper complex of **6**, close approaches are found to the putative coordinated hydroxide by the putative lattice water molecules (O(01)···O(02,03) 2.68(1), 2.61(1) Å. No associated hydrogen atoms were located and there are diverse contacts to the ordered PF_6^- anion; the crystal packing has incipient higher symmetry (Fig. 16). Among the silver complexes, only one is

Table 4 Silver environments, $[AgL]^+$, (L = **2**, **4**, **5** and **6**) and nickel environments $[NiL]^{2+}$, L = **3** and **5**. Presentation as in Table 1. The six values in each entry are for $[Ag(\mathbf{2})]^+$, $[Ag(\mathbf{4})]^+$,[a] $[Ag(\mathbf{5})]^+$, $[Ag(\mathbf{6})]^+$, $[Ni(\mathbf{3})]^{2+}$, $[Ni(\mathbf{5})]^{2+}$ respectively

Atoms	*r*	N(3)	N(3′)	O(5)	O(5′)	N(61)
N(0)	2.455(3)	73.03(11)	74.60(10)	118.38(8)	120.03(8)	176.48(11)
	2.232(2)	(–)	76.49(8)	104.42(7)	106.10(7)	139.85(8)
	2.523(3)	74.86(10)	73.44(9)	90.99(8)	138.05(10)	133.70(8)
	2.425(2)	76.09(7)	70.41(7)	134.09(6)	102.04(6)	160.53(8)
	2.046(3)	83.3(1)	82.2(1)	105.4(1)	99.6(1)	177.5(1)
	2.129(2)	83.80(5)	83.10(5)	105.63(5)	102.07(5)	177.95(6)
N(3)	2.520(3)		147.00(10)	69.95(8)	121.46(8)	103.50(11)
	(3.737(2))		(–)	(–)	(–)	(–)
	2.493(3)		103.35(10)	71.26(8)	133.42(8)	122.47(11)
	2.513(2)		131.45(6)	72.12(6)	156.52(6)	119.35(7)
	2.176(3)		164.8(1)	88.3(1)	98.7(1)	98.1(1)
	2.154(1)		164.75(6)	87.60(4)	100.81(4)	98.06(5)
N(3′)	2.510(3)			133.40(8)	70.90(9)	108.78(10)
	2.508(2)			142.34(6)	78.70(6)	137.32(7)
	2.483(3)			164.42(8)	70.14(8)	129.98(10)
	2.700(2)			108.51(6)	66.77(6)	102.40(7)
	2.107(3)			91.0(1)	88.3(1)	96.5(1)
	2.073(1)			88.44(4)	89.55(5)	95.18(5)
O(5)	2.965(3)				121.11(7)	60.17(8)
	3.061(2)				133.92(5)	63.79(6)
	2.938(3)				124.43(7)	61.82(8)
	2.687(2)				120.07(5)	65.07(6)
	2.130(3)				154.7(1)	76.8(1)
	2.197(1)				151.76(5)	75.37(5)
O(5′)	2.957(3)					61.07(8)
	2.645(2)					70.58(6)
	2.887(2)					64.25(8)
	2.891(2)					58.93(6)
	2.130(2)					78.2(1)
	2.151(1)					76.77(5)
N(61)	2.353(3)					
	2.240(2)					
	2.414(3)					
	2.373(2)					
	2.019(3)					
	2.055(2)					

[a] In $[Ag(\mathbf{4})]^+$, Ag(1′) distances are 2.266(3), 2.565(3), 3.414(3), 2.912(3), 4.985(3), 4.152(3) Å respectively. Ag(1)···Ag(1′) is 2.402(2) Å; Ag(1′) also has contacts to C(32,32′,33′,46) at 2.751(4), 2.472(4), 2.771(4), 3.044(3) Å.

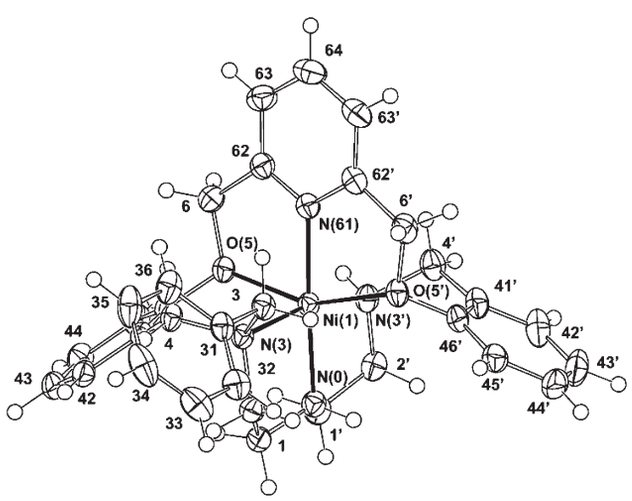

Fig. 14 Projection of the $[Ni(\mathbf{3})]^{2+}$ dication.

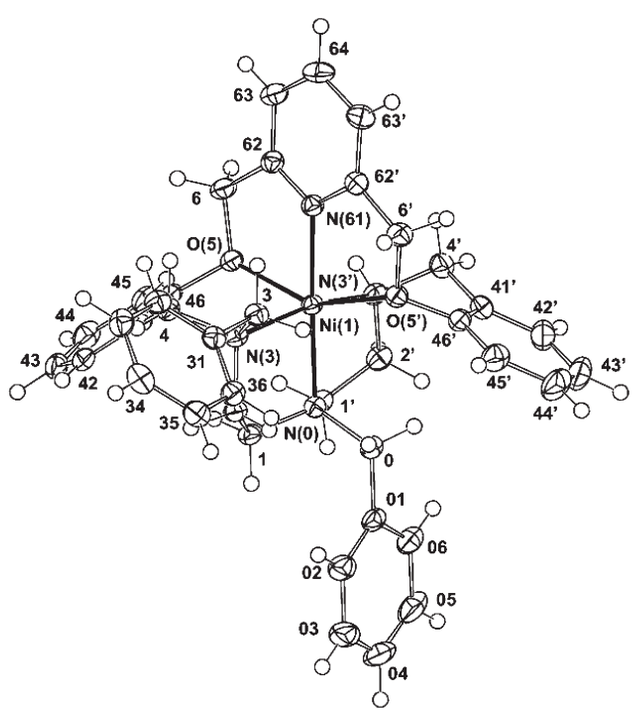

Fig. 15 Projection of the $[Ni(\mathbf{5})]^{2+}$ dication.

solvated $[Ag(\mathbf{6})]PF_6{\cdot}CH_3CN$, the solvent showing high displacement parameters and seemingly having little role in determining the structure, a comment generally true of the quasi-spherical $(XF_n)^-$ anions which, albeit, are in most cases well-ordered, but with high displacement parameters. The NH(3,3′) hydrogens are no longer appropriately oriented for chelation of anion or solvent in either these or the nickel(II) complexes of **3** and **5**.

DFT calculations

As mentioned above, the X-ray structure of $[Ag(\mathbf{4})]PF_6$ shows disorder of the silver over two sites. DFT calculations were carried out to evaluate the relative energies of the two forms as well as to probe the nature of the interaction between the silver ion and the donor atoms and/or the π-faces of particular aromatic rings within the structures. The calculated geometry of

Table 5 Hydrogen-bonding interactions in [M(**2**)$(NO_3)_2$]. Non-hydrogen distances are given for M = Co, Zn, Cd, the second entries (in parentheses) being the refined hydrogen distance[a]

Atoms	Distances/Å		
N(3)(H(3))···O(10)	3.066(2) (2.27(2))	3.056(4)	3.115(2) (2.34(2))
N(3′)(H(3′))···O(10)	3.012(3) (2.32(2))	3.011(4)	3.053(4) (2.35(2))
O(10)(H(10))···N(61)	2.824(3) (2.06(4))	2.827(5)	2.802(3) (2.01(3))
O(20)(H(20))···O(22)	2.878(3) (1.99(5))	2.885(5)	2.839(2) (1.97(4))

[a] In the nickel complex, N(3,3′)···O(10) are 3.102(2), 2.976(2) and O(10)···N(61), O(11) are 2.860(2), 2.848(2) Å.

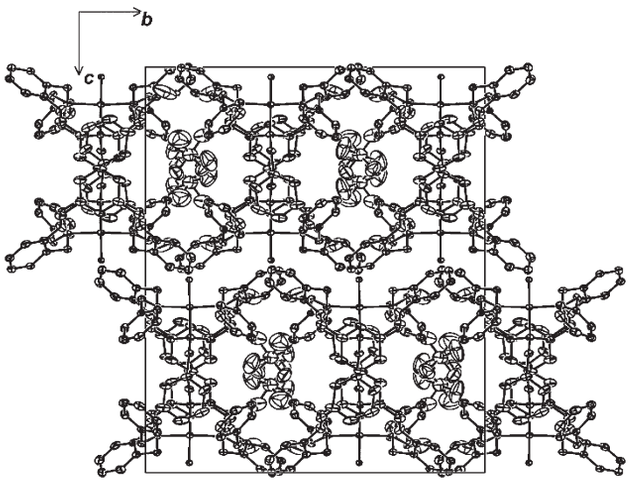

Fig. 16 Unit cell contents of [Cu(**6**)(OH)]PF_6·$2H_2O$ projected down *a*.

the lowest found minimum structure (which corresponds to the 'major' component in the crystal structure) is given in the electronic supplementary information as Fig. S1.† As observed in the crystal structure, this calculated minimum structure shows a distorted four-coordinate array about the silver ion that involves the secondary nitrogen atom, one tertiary nitrogen atom, one pyridine nitrogen atom and one oxygen atom. While two C–H···aryl π interactions are evident (2.65 and 2.81 Å) within the folded ligand structure, the calculated charge distributions indicate that charge transfer from each π region of the aromatic ring to the corresponding C–H group is quite small.

The calculated geometry of the second (minimum energy) structure corresponding to the minor position within the disordered crystal structure is given as Fig. S2.† Once again, the generated structure strongly resembles the X-ray structure. A coordination arrangement in which the silver is bound to the same macrocyclic ligand donors as those observed in the first structure is present; however, in this case one aryl ring also makes a close contact with the metal ion, with an Ag–C distance of 2.45 Å. Previously it has been noted that experimental Ag–C distances in the range 2.45–2.49 Å are typical of η^1 or η^2 coordination in silver–arene complexes,[31] although a η^1 distance as short as 2.40 Å has been reported.[32] The total energy (E_{total}) obtained for this species is 51.5 kJ mol^{-1} larger than for the above lowest energy structure for the major component. Once again, two C–H···aryl π interactions are maintained within the bound ligand superstructure at almost identical distances (2.59 Å, 2.77 Å) to those observed in the structure of the major component. Both C–H···aryl π interactions in each case appear to help define the molecular geometries of the respective [Ag(**4**)]$^+$ cations observed for [Ag(**4**)]PF_6.

Concluding remarks

In the present study the metal complexes of macrocycles **2**–**6** were investigated in the solid state and solution. Collectively, the potentiometric, liquid–liquid extraction and competitive membrane transport studies indicate that the effect of *N*-benzylation of the secondary amine donor groups of **1** to produce **2**–**6** yields an enhanced tendency towards selectivity for silver(I) relative to the other six metals investigated. Such behaviour is thus in accord with the use of selective 'detuning' as a mechanism for achieving metal ion discrimination.[5] Based on the discussion on the effects of *N*-alkylation presented in the Introduction, it appears likely that the origins of the observed behaviour involve a number of influences. Since, *N*-benzylation is involved in the present systems, an additional factor may contribute in such cases. That is, there is a prospect that the relative stabilities of the silver complexes are enhanced by the occurrence of aryl–silver π-interactions in solution; as mentioned already, such interactions have now been well demonstrated for silver(I) in the complexes of a wide variety of aryl-containing ligands.[32–34] However, even though the present X-ray and computational studies suggest that such interactions may occur in the structures of particular complexes in both the solid state and gas phase, in the absence of further evidence it appears inappropriate to comment further on the likely effect (if any) of such π-interactions on the selective detuning behaviour documented in the present report.

Acknowledgements

We thank the Australian Research Council, and the Deutsche Forschungsgemeinschaft for funding to support the collaboration between the research groups involved in this work. We acknowledge Ms U. Stöckgen of TU Dresden for assistance with the radiotracer studies.

References

1 T. W. Hambley, L. F. Lindoy, J. R. Reimers, P. Turner, G. Wei and A. N. Widmer-Cooper, *J. Chem. Soc., Dalton Trans.*, 2001, 614; A. N. Widmer-Cooper, L. F. Lindoy and J. R. Reimers, *J. Phys. Chem. A*, 2001, **105**, 6567.
2 J. Kim, T.-H. Ahn, M. Lee, A. J. Leong, L. F. Lindoy, B. R. Rumbel, B. W. Skelton, T. Strixner, G. Wei and A. H. White, *J. Chem. Soc., Dalton Trans.*, 2002, 3993.
3 M. Fainerman-Melnikova, A. Nezhadali, G. Rounaghi, J. C. McMurtrie, J. Kim, K. Gloe, M. Langer, S. S. Lee, L. F. Lindoy, T. Nishimura, K.-M. Park and J. Seo, *Dalton Trans.*, 2004, 122.
4 Y. Dong, S. Farquhar, K. Gloe, L. F. Lindoy, B. R. Rumbel, P. Turner and K. Wichmann, *Dalton Trans.*, 2003, 1558.
5 L. F. Lindoy, *Pure Appl. Chem.*, 1997, **69**, 2179.
6 A. S. Craig, R. Kataky, R. C. Matthews, D. Parker, G. Ferguson, A. Lough, H. Adams, N. Bailey and H. Schneider, *J. Chem. Soc., Perkin Trans. 2*, 1990, 1523; H.-J. Buschmann, E. Schollmeyer, R. Trueltzsch and J. Beger, *Thermochim. Acta*, 1993, **213**, 11.
7 V. P. Solov'ev, N. N. Strakhova, V. P. Kazachenko, A. F. Solotnov, V. E. Baulin, O. A. Raevsky, V. Rüdiger, F. Eblinger and H.-J. Schneider, *Eur. J. Org. Chem.*, 1998, 1379; R. M. Izatt, K. Pawlak, J. S. Bradshaw and R. L. Bruening, *Chem. Rev.*, 1991, **91**, 1712; R. D. Hancock, *Coord. Chem. Rev.*, 1994, **133**, 39.
8 D. Meyerstein, *Coord. Chem. Rev.*, 1999, **185–186**, 141; G. Golub, H. Cohen, P. Paoletti, A. Bencini, L. Messori, I. Bertini and D. Meyerstein, *J. Am. Chem. Soc.*, 1995, **117**, 8353; G. Golub, H. Cohen, P. Paoletti, A. Bencini and D. Meyerstein, *J. Chem. Soc., Dalton Trans.*, 1996, 2055; G. Golub, I. Zilberman, H. Cohen and D. Meyerstein, *Supramol. Chem.*, 1996, **6**, 275; N. Navon, G. Golub, H. Cohen, P. Paoletti, B. Valtancoli, A. Bencini and D. Meyerstein, *Inorg. Chem.*, 1999, **38**, 3484; T. Clark, M. Hennemann, R. van Eldik and D. Meyerstein, *Inorg. Chem.*, 2002, **41**, 2927.
9 G. J. Kubas, *Inorg. Synth.*, 1979, **19**, 90.
10 R. R. Fenton, L. F. Lindoy, J. R. Price, B. W. Skelton and A. H. White, *Aust. J. Chem.*, 2003, **56**, 1141.

11 *Bruker WINEPR System 2.11 (shareware)*, Bruker-Franzen Analytic GmbH, Bremen, Germany, 1996.
12 P. Gans, A. Sabatini and A. Vacca, *Inorg. Chim. Acta*, 1976, **18**, 237.
13 P. S. K. Chia, L. F. Lindoy, G. W. Walker and G. W. Everett, *Pure Appl. Chem.*, 1993, **65**, 521.
14 D. D. Perrin and B. Dempsey, *Buffers for pH and metal ion control*, Chapman and Hall, London, 1979.
15 S. R. Hall, D. J. du Boulay and R. Olthof-Hazekamp (Editors), *The Xtal 3.7 System*, University of Western Australia, 2001.
16 G. M. Sheldrick, *SHELX97, Programs for Crystal Structure Analysis*, University of Göttingen, Institüt für Anorganische Chemie der Universität, Göttingen, Germany, 1998.
17 *ADF version 1999.02*, Chemistry Department, Vrije Universiteit, De Boelelaan, Amsterdam, 1999; G. T. Velde and E. J. Baerends, *J. Comput. Phys.*, 1992, **99**, 84; C. F. Guerra, J. G. Snijders, G. T. Velde and E. J. Baerends, *Theor. Chem. Acc.*, 1998, **99**, 391.
18 E. J. Baerends, D. E. Ellis and P. Ros, *Chem. Phys.*, 1973, **2**, 41.
19 P. Boerrigter, G. T. Velde and E. J. Baerends, *Int. J. Quantum Chem.*, 1988, **33**, 87; G. T. Velde and E. J. Baerends, *Int. J. Quantum Chem.*, 1992, **37**, 84.
20 A. D. Becke, *Phys. Rev. A*, 1988, **38**, 3089.
21 J. P. Perdew, *Phys. Rev. B*, 1986, **33**, 8822.
22 L. Versluis and T. Zeigler, *J. Chem. Phys.*, 1988, **88**, 322.
23 R. R. Fenton, R. Gauci, P. C. Junk, L. F. Lindoy, R. C. Luckay, G. V. Meehan, J. R. Price, P. Turner and G. Wei, *J. Chem. Soc., Dalton Trans.*, 2002, 2185.
24 W. J. Geary, *Coord. Chem. Rev.*, 1971, **7**, 81.
25 F. A. Cotton, G. Wilkinson, C. A. Murillo and M. Bochmann, *Advanced Inorganic Chemistry*, 6th ed, Wiley, New York, 1999.
26 K. Gloe, P. Muhl and J. Beger, *Z. Chem.*, 1988, **28**, 1 and refs. therein.
27 F. Hofmeister, *Arch. Exp. Pathol. Pharmakol.*, 1888, **24**, 247.
28 C. Chatroux, K. Wichmann, G. Goretzki, T. Rambusch, K. Gloe, U. Muller, W. Muller and F. Vögtle, *Ind. Eng. Chem. Res.*, 2000, **10**, 3616.
29 M. W. Glenny, A. J. Blake, C. Wilson and M. Schröder, *Dalton Trans.*, 2003, 1941.
30 J. Kim, T.-H. Ahn, M. Lee, A. J. Leong, L. F. Lindoy, B. R. Rumbel, B. W. Skelton, T. Strixner, G. Wei and A. H. White, *J. Chem. Soc., Dalton Trans.*, 2002, 3993.
31 F. H. Allen, *Acta Crystallogr., Sect. B*, 2002, **58**, 380.
32 E. A. H. Griffith and E. L. Amma, *J. Am. Chem. Soc.*, 1974, **96**, 743 and refs. therein.
33 K. Shelly, D. C. Finster, Y. J. Lee, W. R. Scheidt and C. A. Reed, *J. Am. Chem. Soc.*, 1985, **107**, 5955.
34 M. Mascal, J.-L. Kerdelhue, A. J. Blake, P. A. Cooke, R. J. Mortimer and S. J. Teat, *Eur. J. Inorg. Chem.*, 2000, 485; A. N. Khlobystov, A. J. Blake, N. R. Champness, D. A. Lemenovskii, A. G. Majouga, N. V. Zyk and M. Schröder, *Coord. Chem. Rev.*, 2001, **222**, 155.